Catalysis Letters 7 (1990) 83–106

CARBIDE PHASES ON IRON-BASED FISCHER-TROPSCH SYNTHESIS CATALYSTS
PART II: SOME REACTION STUDIES

John B. BUTT

Ipatieff Laboratory and Department of Chemical Engineering, Northwestern University, Evanston, IL 60208-3120, U.S.A.

Synthesis catalysts, iron alloy catalysts, phase transitions, iron carbide, iron nitride, selectivity, synthesis reactions

In Part I we have examined some aspects of the characterization and specific reactivity of iron catalysts for synthesis applications, with particular attention to the role of the iron carbide phases that are formed. In this part we continue this examination, but with more attention to reactivity and selectivity than to characterization, and with more attention to iron alloy formulations. However, the role of carbide formation is still an important overall factor in looking at results obtained.

1. Introduction

A few general observations are in order before discussion of detailed results. First is the fact that in FT catalysis there is a net conversion of hydrogen to water. For example, the olefin-forming reaction:

$$2nH_2 + nCO \rightarrow C_nH_{2n} + nH_2O \quad (1)$$

yields 1 mole of water for every mole of carbon entering the chain. The usage ratio of CO to H in FT is determined to some extent by the length of the hydrocarbon chains and the degree of saturation. However, it is generally recognized that water is the initial oxygen-containing product and a dominant factor contributing to this ratio is the secondary water-gas shift reaction:

$$H_2O + CO \rightleftarrows CO_2 + H_2. \quad (2)$$

Here, for every mole of water that is not shifted to CO_2, one more mole of H_2 is consumed, so high water gas shift activity is a desirable feature. This factor is sometimes overlooked in comparison with the obvious importance of α-olefin production; as a result, the conversion dependence of reaction rates and selectivity is a factor of importance.

Following this, some reaction results with the series of iron alloy catalysts (Fe-Ni, Fe-Co, Fe-Cu) and promoted iron (Fe-K), described in Part I, are of

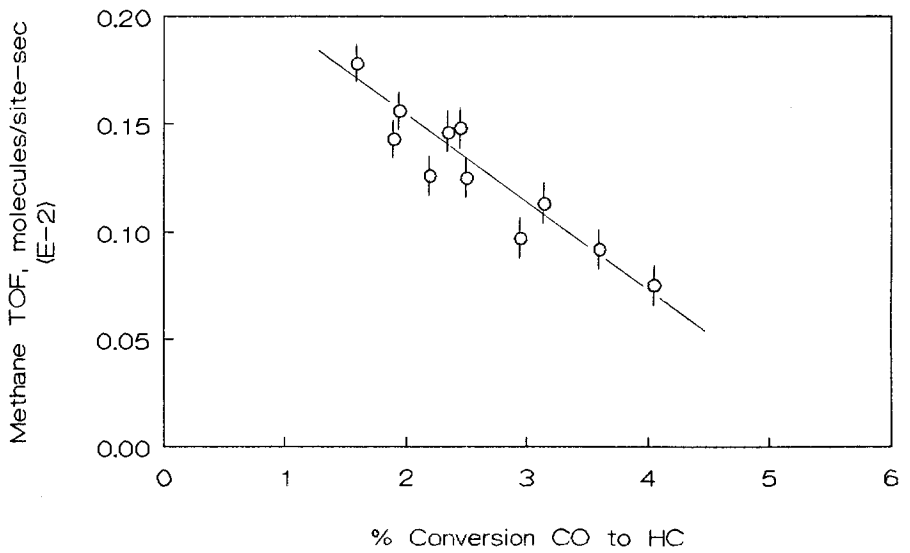

Fig. 1. Conversion dependence of methane turnover frequency (TOF) for Fe-Co-1.

interest. These experiments were most generally conducted at 250°C with $CO/H_2 = 1/3$. Methane turnover frequency *, N_{CH_4} is a convenient if not very sophisticated measure of activity. For pure Ni, Co and Fe-Ni this is independent of conversion (CO to hydrocarbons) up to 6%. However, Fe, Fe-K, Fe-Cu and Fe-Co all show N_{CH_4} sharply decreasing with conversion even over this limited range, probably due to product inhibition by water. The behavior appears more correlated with the adsorptive properties of Fe rather than carbide. A typical example of the magnitude of such inhibition is shown in fig. 1. Further to the question of FT efficiency is the CO_2/H_2O ratio, which can be taken as a measure of shift activity, with a higher ratio at a given conversion indicative of higher shift activity. The comparisons here are given in fig. 2, where the big winners with respect to Fe are Fe-K and Fe-Co; Fe-Ni is poorer but dependent upon composition, and Fe-Cu (not shown) about the same as Fe. Since Fe-K carburizes completely and Fe-Co not at all under these conditions the increase in shift activity would appear to be due to electronic interaction between the alloying component and Fe, much as has been described for uncarburized Fe-K. Further comparison also shows that those catalysts that do not show high shift activity are also those not inhibited by product water formation, however. Fe-Co is of particular interest, since the shift activity of pure Co is very small and is well correlated with the small chemisorption of water on this metal [2].

* Determination of specific rates (i.e., turnover frequencies per surface Fe atom here) depends upon a means for measurement of exposed iron surface. A convenient method based on hydrogen desorption is described in [1,5].

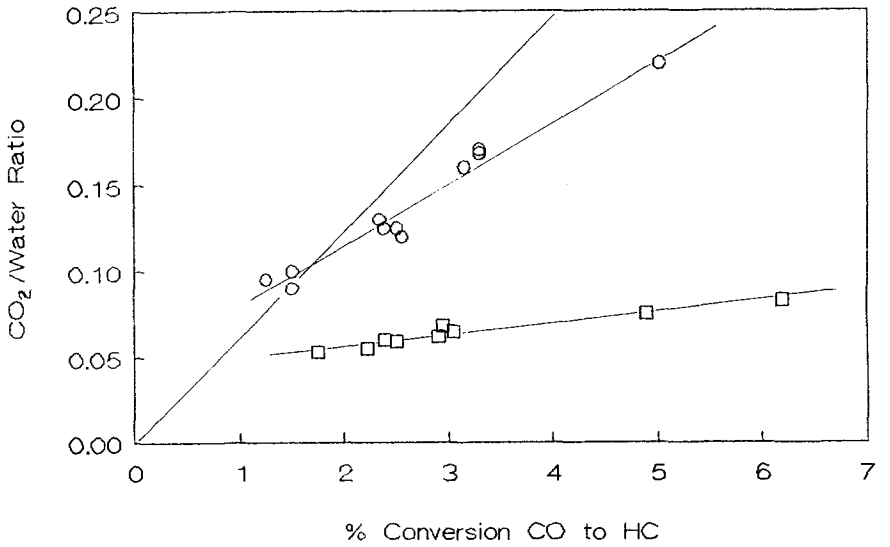

Fig. 2a. Conversion dependence of the CO_2/H_2O ratio for Fe-Ni-1 and Fe-Ni-2. ○ – Fe-Ni-1 (Fe/Ni = 4.3), □ – Fe-Ni-2 (Fe/Ni = 1.0). Solid line – reference for Fe.

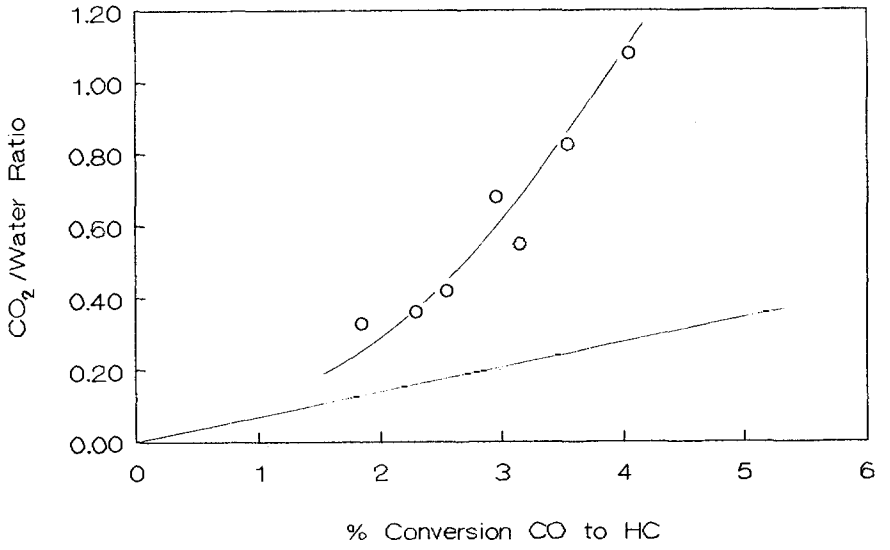

Fig. 2b. Conversion dependence of the CO_2/H_2O ratio for Fe-Co-1 (Fe/Co = 3.98). Solid line – reference for Fe.

In addition to N_{CH_4} and CO_2/H_2O, a third figure of merit is the conversion dependence of the olefin/paraffin ratio, which is a measure of the relative importance of olefin hydrogenation and incorporation into growing chains. Relative to the base Fe/SiO_2 catalyst, of interest are Fe-Co which exhibits the highest olefin/paraffin ratio, Fe-K which shows the highest tendency to form high molecular weight hydrocarbons and is an efficient olefin maker, and Fe-Ni

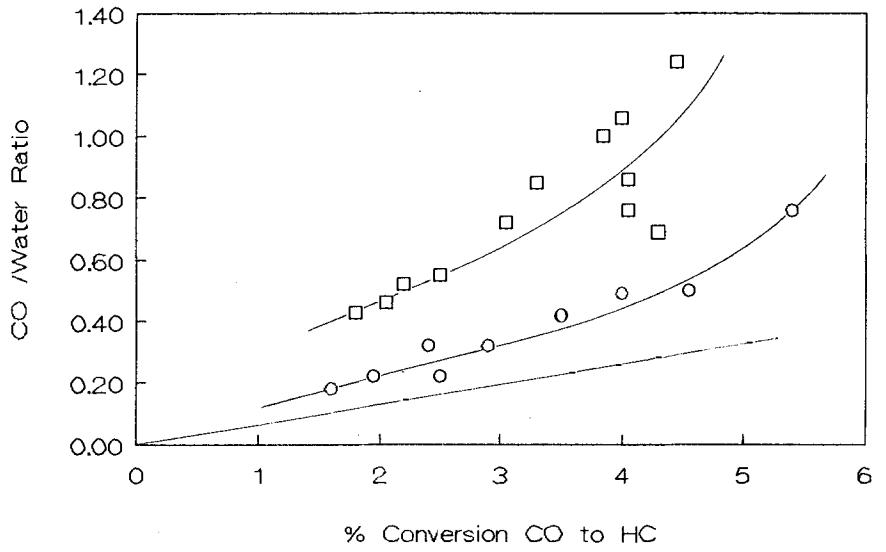

Fig. 2c. Conversion dependence of the CO_2/H_2O ratio for Fe-K-1 and Fe-K-2. ○ – Fe-K-1 (4.94% Fe), □ – Fe-K-2 (9.96% Fe). Solid line – reference for Fe.

which exhibits the lowest olefin/paraffin ratio. A wide range of behaviors is found here; comparisons are given in fig. 3 for $C_2^=/C_2$ with similar comparative behavior for $C_3^=/C_3$. Incompletely carburized Fe has a lower hydrogenation potential (higher olefin/paraffin ratio) than the fully carburized material, hence the tendency of carbide formation alone is to diminish this desirable selectivity property. However, the potassium promotion is more than enough to compensate

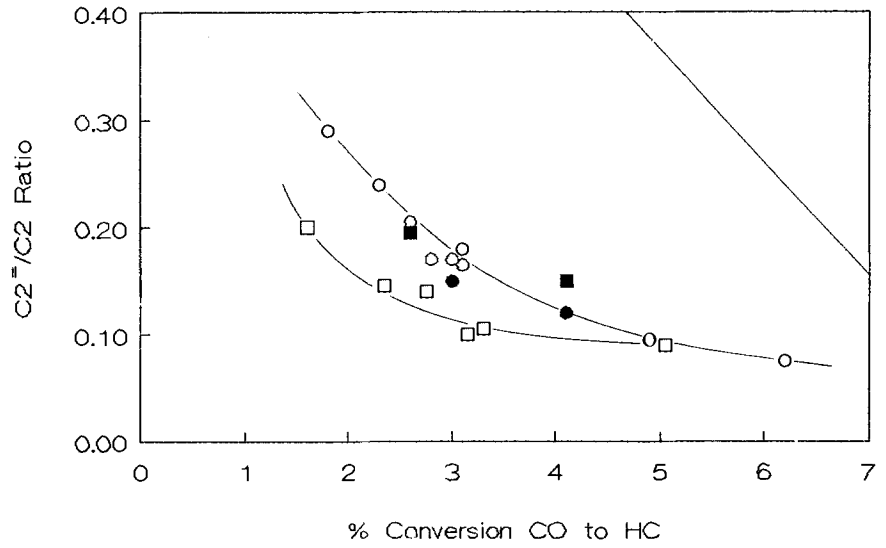

Fig. 3a. Conversion dependence of the $C_2^=/C_2$ ratio for Fe-Ni-1 and Fe-Ni-2. ○ – Fe-Ni-1, □ – Fe-Ni-2. Darkened points represent time = 6 min. Solid line – reference for Fe.

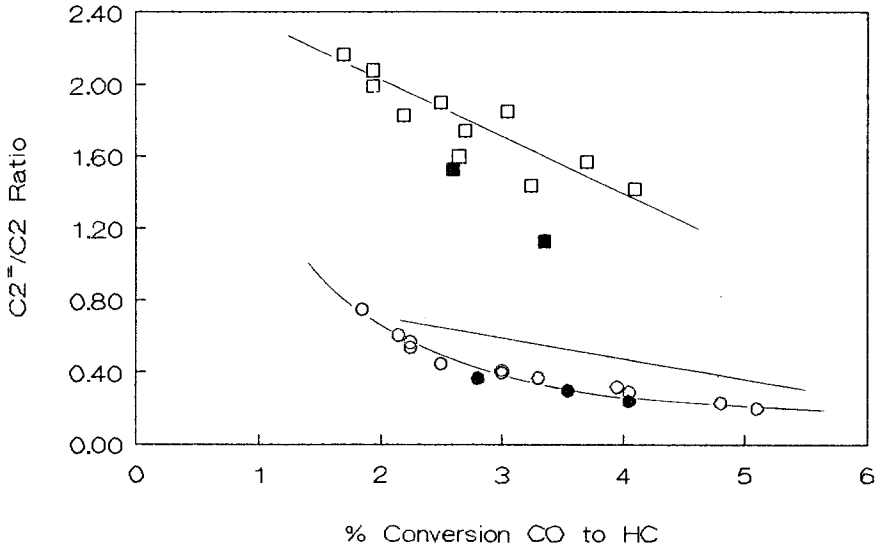

Fig. 3b. Conversion dependence of the $C_2^=/C_2$ ratio for Co and Fe-Co-1. ○ – Co, □ – Fe-Co-1. Darkened points represent time = 6 min. Solid line – reference for Fe.

for this undesirable property of the carbide, as shown in fig. 3c. The influence of carbide on olefin formation has been postulated long ago by Podgurski et al. [3] as the result of inhibition of CO chemisorption; the surface of the incompletely carburized catalyst would be covered with a higher CO/H_2 ratio than the carburized material, hence the higher olefin content. This type of relationship has already been indicated by the XPS studies of Part I.

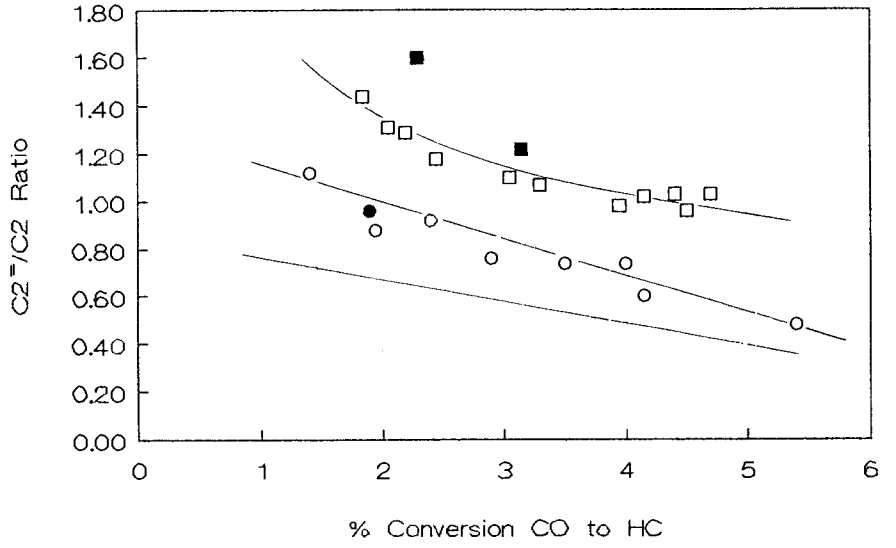

Fig. 3c. Conversion dependence of the $C_2^=/C_2$ ratio for Fe-K-1 and Fe-K-2. ○ – Fe-K-1, □ Fe-K-2. Darkened points represent time = 6 min. Solid line – reference for Fe.

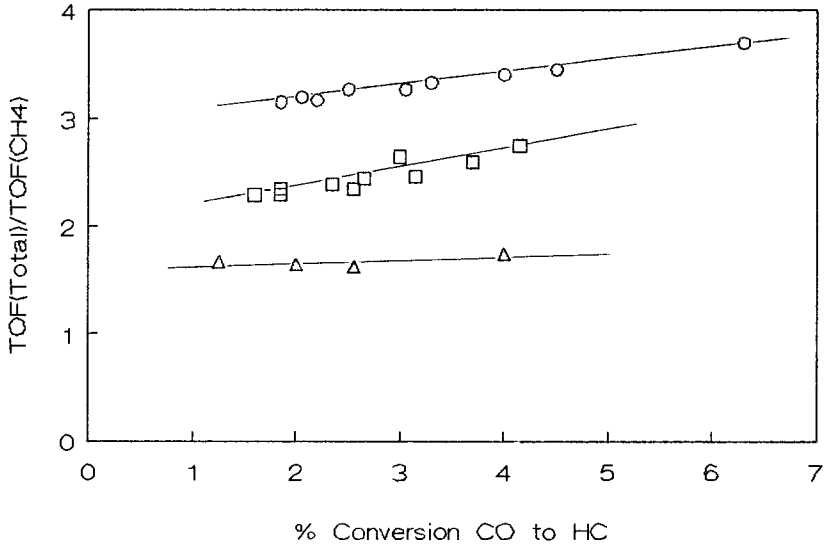

Fig. 4. Conversion dependence of the ratio of total turnover frequency, TOF (total), to methane turnover frequency, TOF (CH_4). ○ – Fe-K-2, □ – Fe-Co-1, △ – Ni-1.

A final comparison which may yield some insight into the role of carbide in the behavior of these catalysts is the selectivity to formation of higher hydrocarbons, given in approximate measure by the ratio of the total turnover frequency for hydrocarbon formation (to C_5) to that for methane formation, N_{TOT}/N_{CH_4}. This comparison is shown in fig. 4. Here the preferred materials are two that might be expected, Fe-K and Fe-Co (high activity and high olefin/paraffin ratio), and one that is not, Ni (with Fe-Ni not far away), in spite of its low olefin/paraffin ratio. The Fe-K forms a carbide in which Fe-C bonds are covalent and highly directional, but one may think of carbon as tending to fill the d-band in iron. This may be reflected overall in the fact that while Fe-K has the highest intrinsic ability to form hydrocarbons, its ability to incorporate initial products into growing chains is not as great as that of Fe-Co, thus the different slopes for the two in fig. 4. Ultimately, the success of Fe-Co is the production of a catalyst with limited hydrogenation activity, electronically akin to Co since the material does not carburize. Ni also does not carburize under these conditions [4].

There are also some aspects of the kinetics of carbide formation that find place in this discussion. As stated early on, the transient activity of supported Fe is correlated with the rate of carbide formation [5,6]. The following sequence has been postulated to explain this:

$$CO + H_2 \rightarrow C_s + H_2O \tag{3}$$

and

$$C_s \begin{matrix} \text{Hydrocarbons} & (k_1) \\ \text{Carbide} & (k_2) \end{matrix} \tag{4}$$

where C_s is some surface intermediate. For the iron catalysts k_2 is evidently greater than k_1 and the surface intermediate forms carbide preferentially. After carburization, only the path to hydrocarbons remains and the FT activity then attains steady state. What of Co/SiO_2, Ni/SiO_2 and the corresponding Fe-Co and Fe-Ni? The first three of these do not form carbides in $1/3:CO/H_2$, but both Ni/SiO_2 and Co/SiO_2 do form carbides in pure CO. For these elements then, both of the pathways in (4) must exist, and the reason for suppression of carbide formation under nominal FT conditions is a kinetic one; i.e., $k_1 \gg k_2$. Partial curburization of Fe-Ni is observed [4], so for this alloy one would conclude that $k_1 \sim k_2$.

The behavior of Fe would appear to play a pivotal role in carbide formation in these alloy systems, if one accepts the general picture of (4). For pure iron, the rate of carburization in $1/3:CO/H_2$ is more rapid than in pure CO, which indicates that the rate of carbide formation is not limited by the diffusion of carbon into the bulk, but rather by a surface reaction. There are only two ways that hydrogen could assist carbide formation: (i) the rate-controlling step involves the removal of oxygen by hydrogen following CO decomposition or (ii) it involves hydrogen reaction with a CO molecule forming an oxygen-containing intermediate. Since the latter seems an unlikely intermediate for carbide formation one is left with the conclusion that oxygen removal is the rate-limiting step for the formation of carbide with iron catalysts in pure CO. When H_2 is present, this may not be the case. Dwyer and Somorjai [7] report that oxygen removal from single iron crystals is rapid in the presence of hydrogen. It is generally accepted, at least for Fe, that the rates of carbide formation and hydrocarbon formation are limited by the same process, and if hydrogenation of surface carbon is ruled out as the rate-limiting step for hydrocarbon formation (which seems likely [1,8]) it would appear that in the presence of hydrogen CO bond breaking controls both of these reactions.

2. Some characteristics of the Fe-Co system

Although the $Fe\text{-}Co/SiO_2$ system does not form a carbide, the topic of this paper, there are some interesting things to be learned from the behavior of Fe-Co in comparision to Fe that are relevant both to the role of electronic promotion (indicated via Mössbauer spectra) and carbide in synthesis.

First of these is the reactive performance at higher pressures, specifically investigated by Arcuri et al. [9]. Two questions come to mind: (i) is there evidence for carbide formation at higher pressure and (ii) what happens to the selectivity patterns (recall this system was particularly good for olefin/paraffin selectivity at 1 atm) at high pressures?. The answer to (i) is that even up to 15 atm and even with $1/1:CO/H_2$ there is no evidence of carbide formation in supported Fe-Co. The implication is that simple pressure forcing does little to alter the kinetics set

by the intrinsic values of k_1 and k_2 in (4). This is of course specific to the Fe-Co system in the range of 250–300°C and 15–20 atm, but it is reasonable to suspect the implication is subject to some generalization. Interestingly, however, the catalyst activity in terms of CO turnover frequency is correlated by an expression proposed for Fe at higher conversions and pressures greater than one atm [10–12].

$$N_{CO} = \frac{kP_{CO}P_{H_2}}{P_{CO} + bP_{H_2}} \tag{5}$$

where N_{CO} is the CO turnover frequency. The answer to (ii) is not a promising one. The image of high olefin selectivity so promising at 1 atm is severely tarnished at higher pressures, as shown in fig. 5 (cf. fig. 3b). Now Fe-Co is poorest of the three among Co, Fe and Fe-Co, and the role of carbide here appears to be only that of stabilization of hydrogenation activity of Co and Fe with pressure. Correlation of chain growth according to the Schulz-Flory-Anderson model is also found:

$$\ln Y_j = n \ln \alpha + \ln \phi \tag{6}$$

where Y_j is the product yield (relative to CO reacted), n the number of carbon atoms in the product j and α the growth probability parameter. These data are shown in fig. 6. The upshot of the matter is that in terms of CO conversion and chain growth probability the alloy catalyst resembles Fe/SiO_2 at atmospheric pressure and Co/SiO_2 at higher pressure. On the other hand, methanol production from the alloy strongly resembles that from Fe at higher pressure, as shown

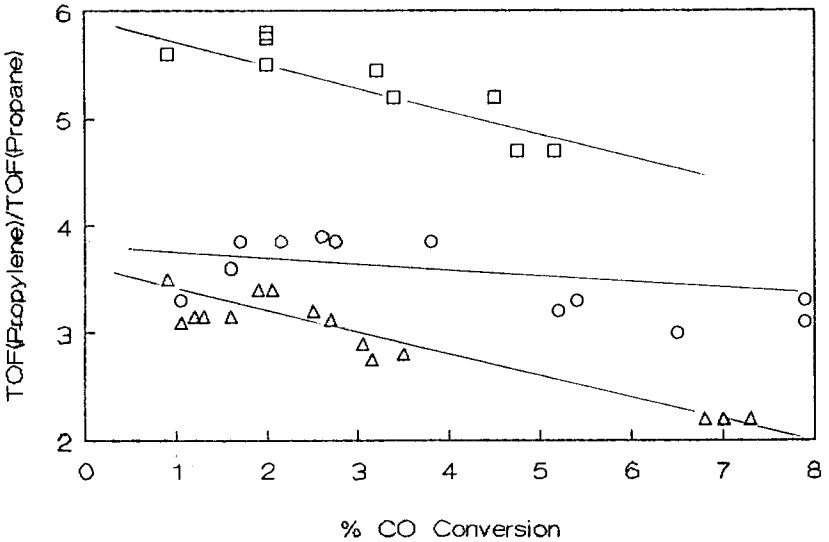

Fig. 5a. Propylene selectivity vs. CO conversion for Fe, CO and FeCO catalysts at 14 atm, 1:3 CO/H_2 feed at 250 °C. ○ – Fe, △ – FeCO, □ – CO.

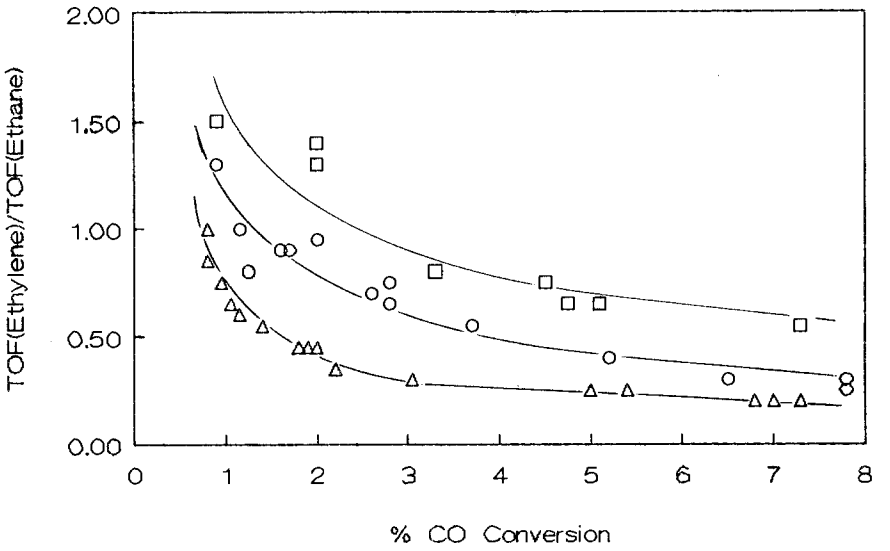

Fig. 5b. Ethylene selectivity vs. CO conversion for Fe, CO and FeCO catalysts at 14 atm, 1:3 CO/H_2 feed at 250 °C. Legend as for fig. 5a.

in fig. 7. This increase in oxygenate selectivity at higher pressures is associated with the presence of Fe^{2+}, stabilized by higher concentrations of H_2O and CO_2 [13,14]. Thus the carbide formation in the iron does not prevent formation of Fe^{2+} under the appropriate conditions.

A final point of comparison between Fe/SiO_2 and $Fe\text{-}Co/SiO_2$ has to do with the long-term trends in activity and selectivity. The data above are for run

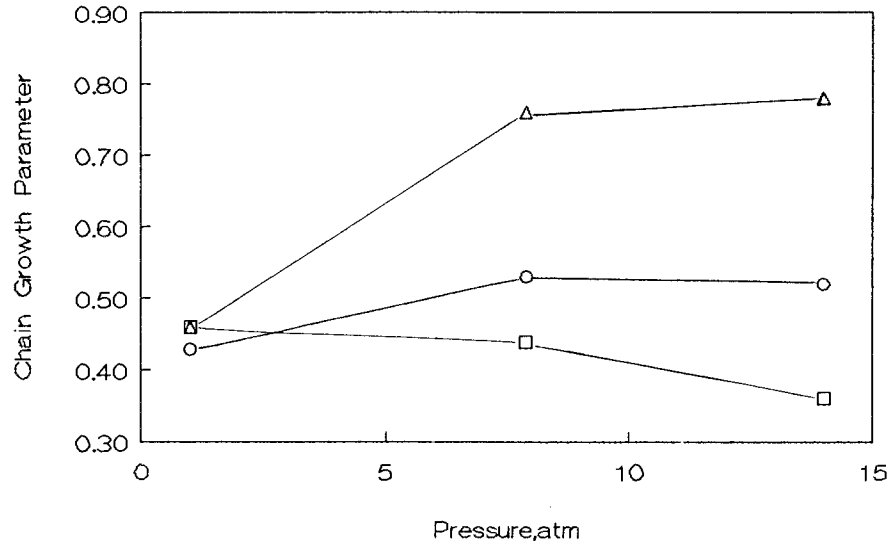

Fig. 6a. Growth probabilities as a function of pressure for 1:3 CO/H_2 feed mixture. △ – Co, ○ – Fe, □ – FeCo.

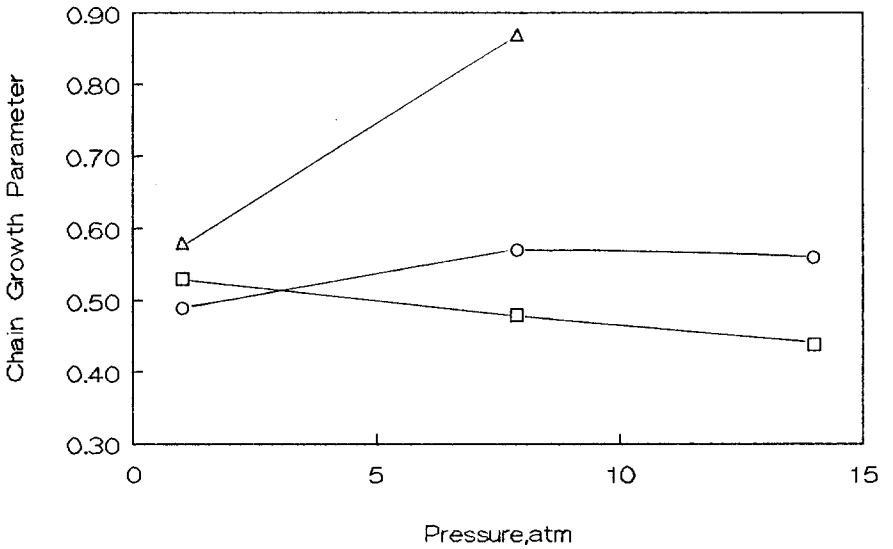

Fig. 6b. Growth probabilities as a function of pressure for 1:1 CO/H_2 feed mixture. Legend as for fig. 6a.

durations of ca. 2–5 h; trends for time-on-stream up to 200 h are given by Butt et al. [15] for experimental conditions comparable to figs. 5–7. The Fe-Co does not deactivate *at all* over the 200 h period, and there is an increase in shift activity and methanol production with time. By contrast Fe/SiO_2 deactivates significantly (after an initial period of activation) over the first 60 h of the run, then becomes stabilized. During the period of deactivation for the Fe/SiO_2 there is a significant

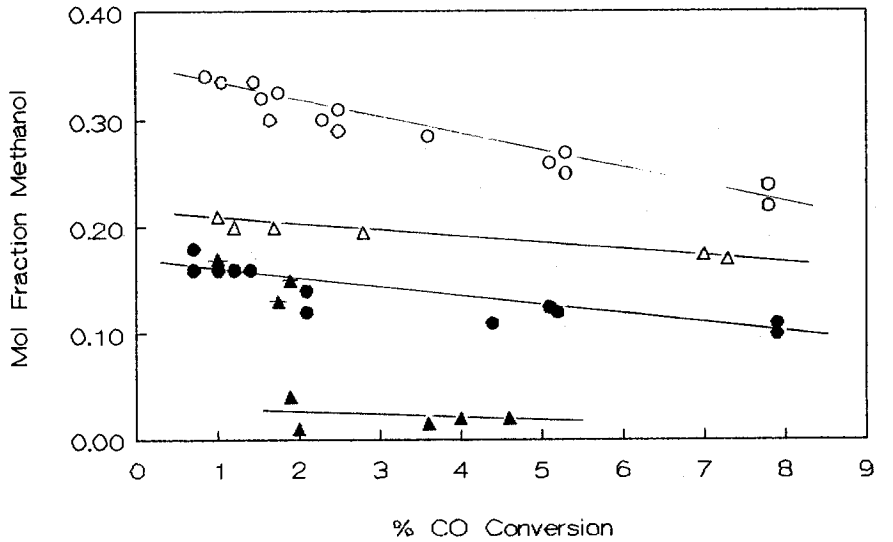

Fig. 7. Product methanol mol fraction vs. CO conversion with 1:3 CO/H_2 feed at 250 °C. ● ○ – Fe at 7.8, 14 atm, ▲ △ – FeCo at 7.8, 14 atm, ▲ – Co at 14 atm.

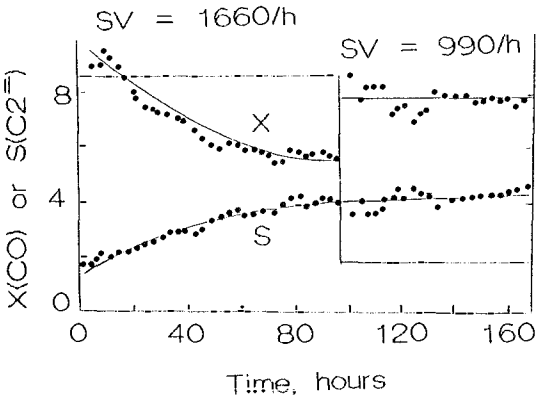

Fig. 8a. Carbon monoxide conversion and ethylene selectivity for Fe/SiO_2 at 250 °C.

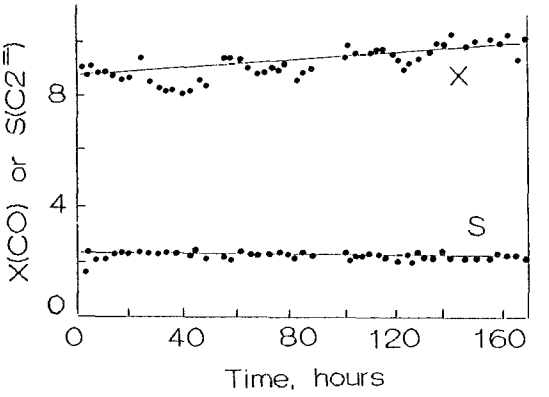

Fig. 8b. Carbon monoxide conversion and ethylene selectivity for $FeCo/SiO_2$ at 250 °C.

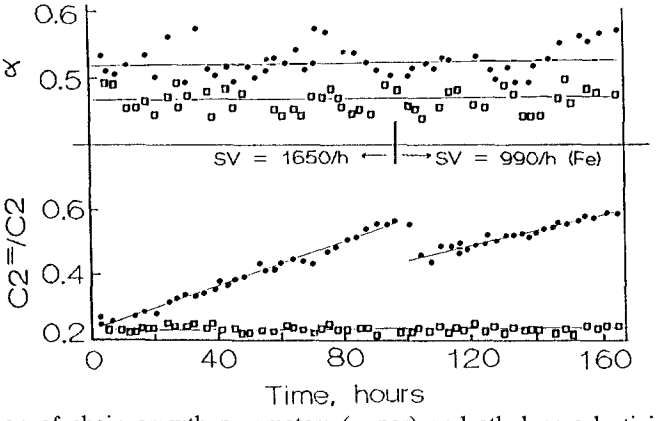

Fig. 8c. Comparison of chain growth parameters (upper) and ethylene selectivity. ● – Fe/SiO_2, □ – $FeCo/SiO_2$.

increase in selectivity for $C_2^=$ (defined as carbon converted to $C_2^=$/carbon reacted in CO). These trends are summarized in fig. 8. Also shown are the chain growth parameter, α, and the $C_2^=/C_2$ ratio for the two catalysts. Overall, the Fe-Co is a

quite stable material; the extent of interaction between the two elements appears set by the conditions of catalyst preparation and is not significantly altered by the FT reaction conditions. By contrast, the Fe/SiO_2 is a rather dynamic material and, at least by some measures (shift activity, $C_2^=$ selectivity, $C_2^=/C_2$ ratio) actually improves with age. The overall data of fig. 8 do not tell us whether these dynamics are related to carbide formation and/or stability (XPS studies have something to say about this, as seen in Part I) but certainly there appears to be some evolution of k_1 and k_2 values in the picture of scheme (4).

3. Carbide formation and characterization in some more-complex systems: FeN and FeMn

The literature is full of reports on catalysts developed for specific selectivities in FT applications, as witness the figures of merit used in the above discussion of Fe and Fe-Co. Two additional systems are of interest in this regard: FeN for its reported high oxygenate (alcohol) selectivity and FeMn for the production of short chain olefins. In some aspects these systems are more complicated than the alloys discussed so far, both with respect to phase composition and carbide formation and stability. The following presents a survey of some of the most important aspects of the characterization and applications of these two systems.

IRON NITRIDE

The generic term "iron nitride" (like "iron carbide") needs to be refined somewhat, since in FT applications, at least with supported catalysts, one is dealing with a system generally categorized as ϵ-Fe_xN, with $2 < x < 3$. In this phase the Fe atoms are arranged as hcp with N atoms occupying the octahedral interstices between the Fe layers. A general discussion of the various iron nitride phases has been given by Jack [16], and a proposed structure for ϵ-Fe_2N is given by the same author [17]. Detailed Mössbauer, magnetic and X-ray characterizations of the ϵ phase have been reported by Chen et al. [18] and these have pertinence because such may be considered to be the starting material for iron nitride FT catalysts.

Under reaction conditions we write the catalyst composition in general as Fe_x $(C_{1-y}N_y)$ and seek the variation of x and y with time-on-stream. Such time-on-stream data are particularly important in this case to determine if (or the extent of) there is replacement of interstitial N by C, and what effect this has on activity/selectivity. A typical catalyst can be prepared by iron impregnation from nitrate onto SiO_2, reduction in H_2, 425°C, 24 h and treatment with NH_3, 495°C, 12 h. The result is ϵ-$Fe_{2.08}N$ [19]. The exposure of this catalyst to synthesis conditions ($CO:/H_2 = 1/3$, $T = 250$°C, $P = 7.8$ atm) results in a relatively rapid displacement of N from the catalysts; the catalyst phase becomes iron-rich during the first three hours in this environment, indicating that N is removed more

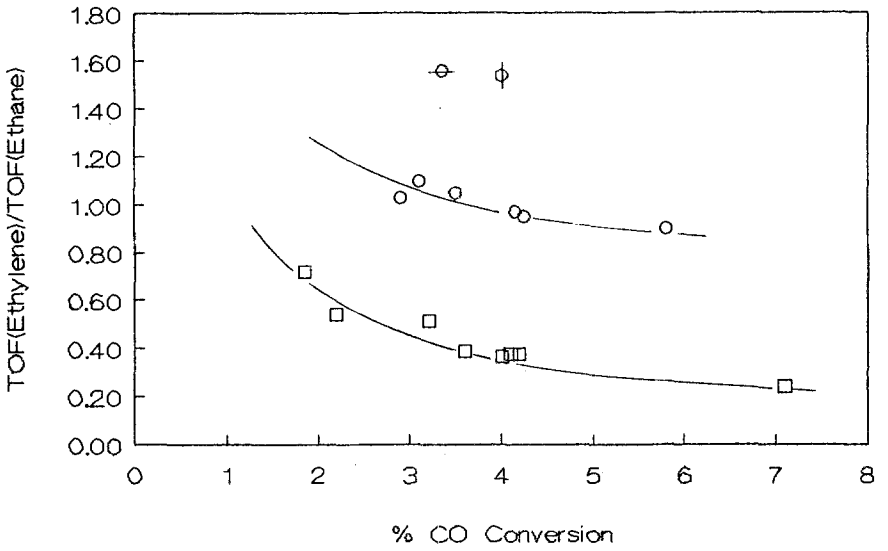

Fig. 9a. Ethylene selectivities vs. conversion for 1:3 feed, 250°C, 14 atm. ○ – Fe nitride, □ – Fe carbide, ϕ – after 18 min, ⊖ – after 64 min.

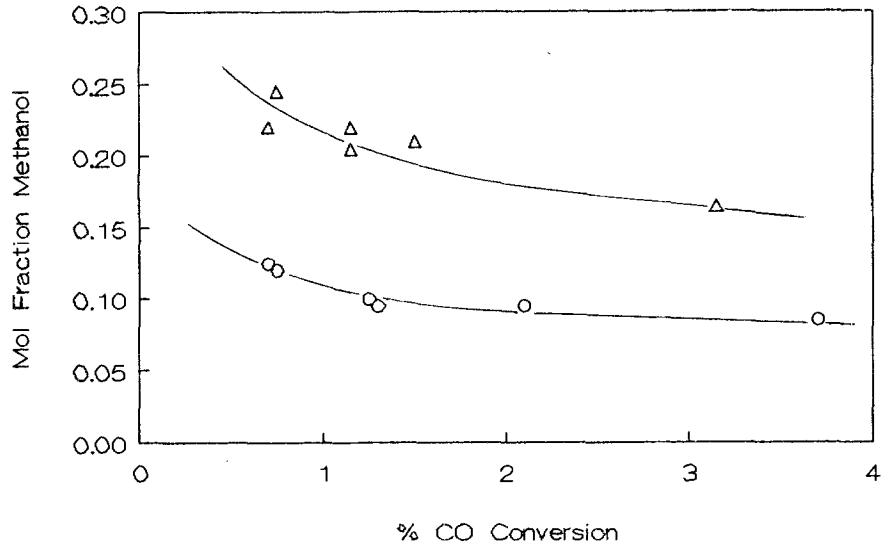

Fig. 9b. Methanol mol fraction vs. CO conversion for 1:1 feed at 7.8 atm △ – Fe carbide, ○ – Fe nitride.

rapidly by H_2 than it is replaced by carbon. After ~ 3 h on stream carburization becomes dominant and the catalyst composition becomes stable after ~ 20 h under these conditions. Not all of the nitrogen is removed, the equilibrium catalyst composition is about $Fe_{2.18}C_{1-y}N_y$ with y between 0.13 and 0.20. Even though small particles are involved here (~ 10 nm) the results are consistent with

the ternary phase diagram for Fe-N-C [20] and the major effect of N on the catalyst (solid) phase behavior is just to inhibit carburization.

Even though most of the nitrogen is eventually replaced by carbon in the equilibrated catalyst (termed Fe-nitride, although the working catalyst is a carbo-nitride), there is still a significant difference in the behavior relative to that of Fe (termed Fe-carbide) as shown in fig. 9 for olefin selectivity and methanol

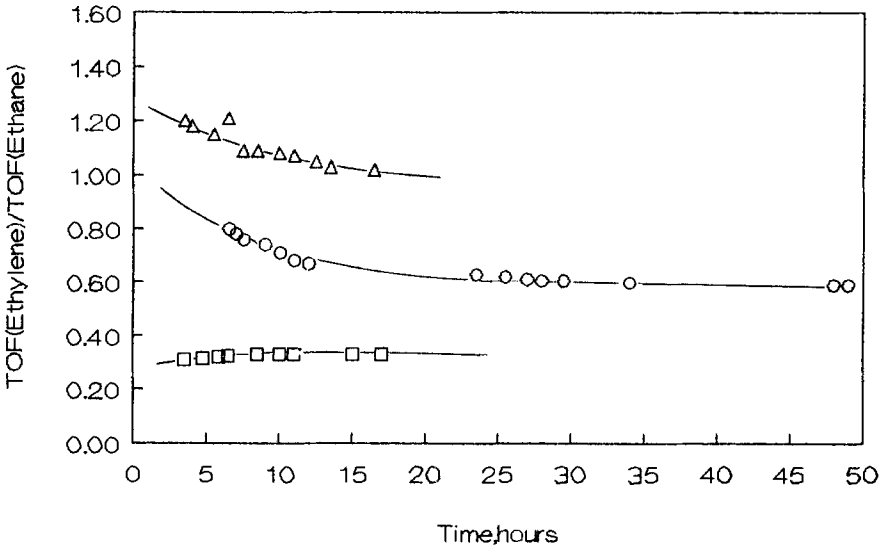

Fig. 10a. Ethylene selectivity as a function of time-on-stream, 1:3 feed, 7.8 atm. △ – Fe-K-nitride, 7.6% conversion, GHSV = 240, ○ – Fe-nitride, 8.5% conversion, GHSV = 255, □ – Fe-carbide, 8.7% conversion, GHSV = 255.

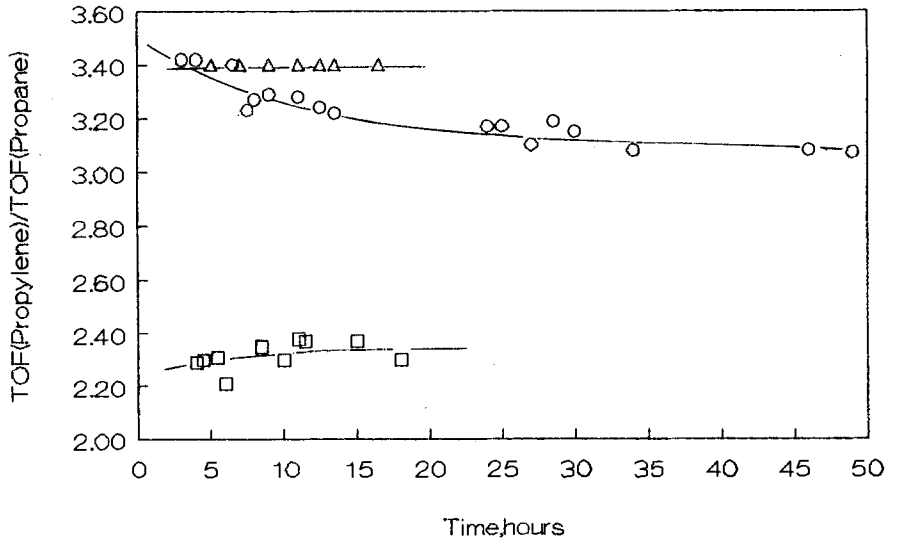

Fig. 10b. Propylene selectivity. Conditions and legend as for fig. 10a.

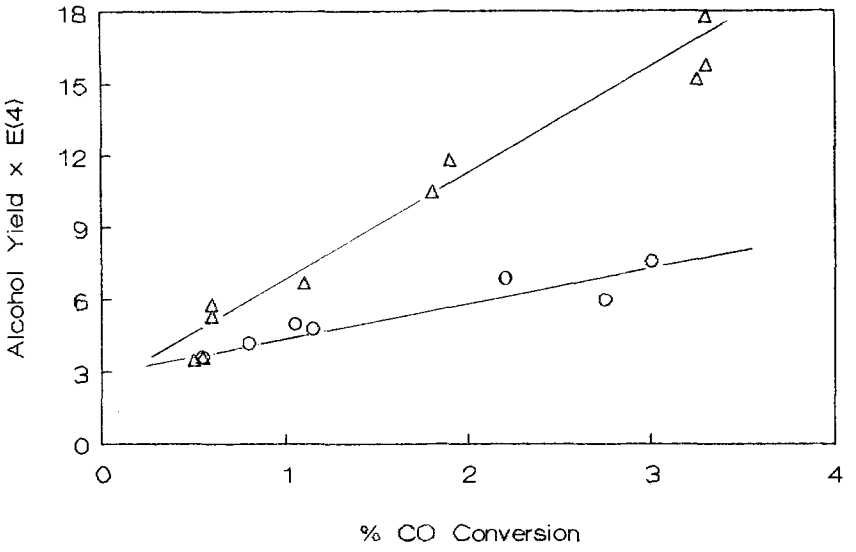

Fig. 11a. Total alcohol yield vs. CO conversion for 1:1 feed at 14 atm. △ – Fe-carbide, ○ – Fe-nitride.

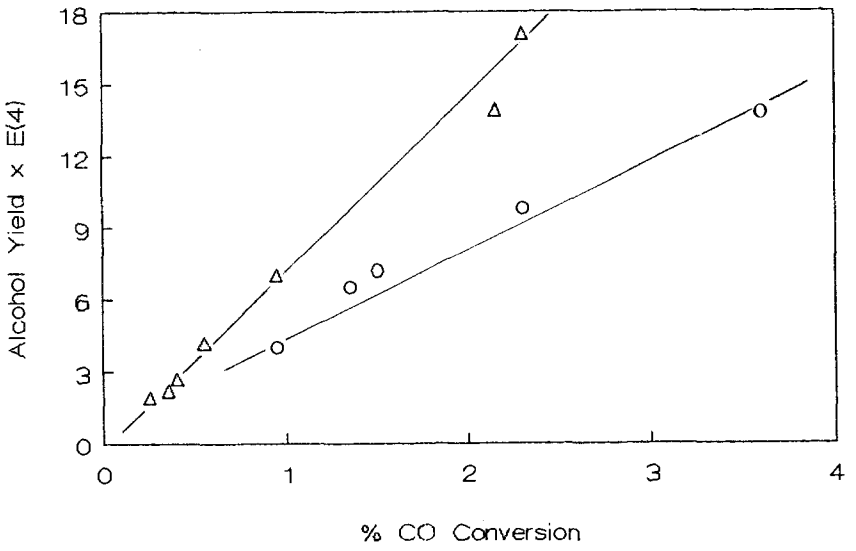

Fig. 11b. Total alcohol yield vs. CO conversion for 1:1 feed at 14 atm, SV=1140/h. △ – Fe-K-carbide, ○ – Fe-K-nitride.

production. There is an apparent (and somewhat unexpected) promotion of ethylene selectivity by nitride relative to carbide, and the points labeled ϕ and θ in fig. 9a indicate that the ϵ-nitride phase before carburization must indeed have very high olefin selectivity with significant inhibition of the hydrogenation activity by the formation of this phase. The alcohol results (fig. 9b), though, are somewhat disappointing, particularly in view of early claims for unsupported

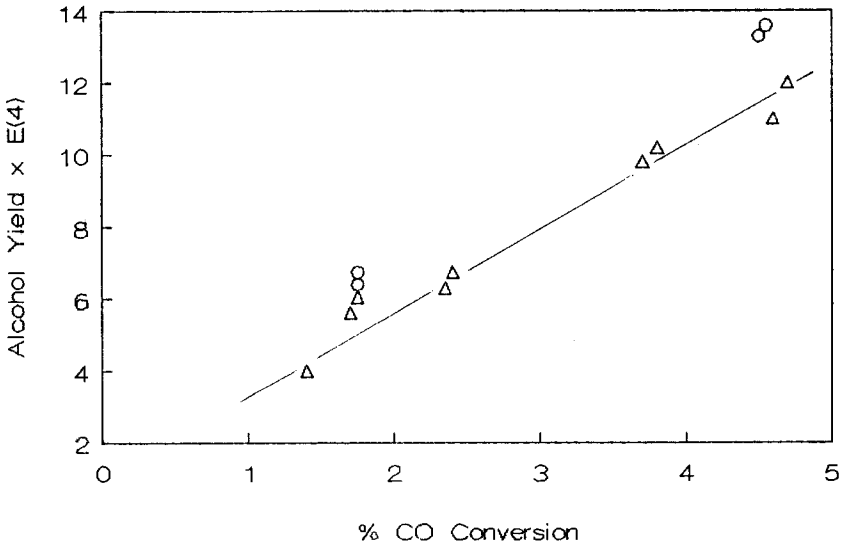

Fig. 11c. Alcohol yield for 1 : 3 feed at 14 atm. △ – Fe-K-carbide, ○ – Fe-K-nitride.

Table 1a
Chain growth parameters, α, for Fe-carbide and Fe-nitride catalysts

Catalyst:	Fe-carbide		Fe-nitride	
Feed (CO/H_2):	1/3	1/1	1/3	1/1
P (atm)				
1	0.554 (5.4) [a]	0.607 (1.8)	0.595 (3.9)	0.619 (1.3)
	0.521 (1.5)	0.601 (0.8)	0.525 (1.2)	0.610 (0.3)
7.8	0.597 (7.8)	0.645 (3.3)	0.651 (5.6)	0.665 (3.7)
	0.590 (2.9)	0.638 (1.2)	0.645 (2.1)	0.654 (0.9)
14	0.607 (7.1)	0.650 (3.5)	0.654 (7.2)	0.670 (4.2)
	0.590 (1.9)	0.630 (1.1)	0.649 (3.5)	0.661 (1.1)

[a] Values in parenthesis are %CO conversion.

Table 1b
Chain growth parameters, α, for Fe-K-carbide and Fe-K-nitride catalysts

Catalyst:	Fe-K-carbide		Fe-K-nitride	
Feed (CO/H_2):	1/3	1/1	1/3	1/1
P (atm)				
1	0.578 (4.5) [a]	0.636 (1.3)	0.637 (5.0)	0.666 (1.8)
	0.497 (1.7)	0.607 (0.5)	0.587 (1.6)	0.587 (0.3)
7.8	0.620 (4.9)	0.629 (1.5)	0.694 (4.8)	0.723 (2.9)
	0.590 (1.5)	0.620 (0.8)	0.684 (1.9)	0.686 (0.6)
14	0.621 (4.7)	0.654 (3.0)	0.699 (4.5)	0.736 (3.4)
	0.613 (1.4)	0.634 (1.0)	0.682 (2.9)	0.691 (1.6)

[a] Values in parenthesis are %CO conversion.

catalysts [21]. Since the Fe-nitride activities are also lower than those of Fe-carbides [22], the net yields of alcohol are also considerably lower. A closer look at that "early work", however, reveals that the bulk nitrided catalysts investigated contained K_2O as one of the ingredients [21,23]; so proper comparison should then probably be made with Fe-K-carbide and Fe-K-nitride.

The K-containing catalysts were prepared as their counterpart Fe-nitride and Fe-carbide, but with coimpregnation of potassium carbonate with iron nitrate to give a K/Fe molar ratio of 0.0175. The K-series catalysts show high performance both with respect to olefin selectivity, fig. 10, and alcohol yield, fig. 11. The Fe-K-nitride has the highest low molecular weight olefin selectivity of all the catalysts investigated in this series, with the indication that the long-term maintenance of selectivity (> 15 h) is very good. For the alcohol yield, it is seen that the K-nitride and K-carbide are approximately the same with 1/3 feed, K-carbide is a little better with 1/1 feed (fig. 11b), but neither of these offers any significant improvement over the basic Fe-carbide (fig. 11a). Unfortunately, the detailed composition and phase behavior data are not available to make a comparison with the unsupported catalysts detailed in refs. [21,23]. However, while the improvement in oxygenate production is questionable, there is no doubt of better olefin selectivity. Finally, there is a significant increase in the chain growth parameter, α, for the nitrided catalysts, as shown in table 1 [22]. The highest α values are seen to belong to the Fe-K-nitride catalysts, indicating an additivity of the effects of potassium and nitrogen in the overall product distribution.

A summary of the observations for this interesting system provides some perspective. In comparison with prior results for Fe-carbide, both Fe-nitride and Fe-K-carbide catalysts have (1) higher olefin selectivity, (2) higher watergas shift activity, (3) equal or lower alcohol yield and (4) a tendency to shift products to higher molecular weight. These tendencies are further enhanced for the Fe-K-nitride catalyst, with the possible exception of point (3). From such observations on the behavior of both K-promoted and nitrided catalysts, one may well wonder whether potassium and nitrogen are doing the same thing. Certainly this seems so from operational experience.

Some evidence was given in Part I supporting the contention that potassium donates electrons to iron [24]. Corresponding studies of iron nitride have shown that nitrogen also donates electrons to iron [18,25,26], in semiquantitative agreement with the donor model of Wiener and Berger [27]. Interpretation of the change in Mössbauer hyperfine field with the number of metalloid (C, N) neighbors in Fe [18,28] suggests that the charge transfer into the partially filled iron 3d band is larger for interstitial nitrogen than for interstitial carbon. * The

* The electron donation from interstitial nitrogen is different from (but not inconsistent with) the case of chemisorbed nitrogen on an iron surface where it is believed to accept electrons from iron. The interstices are too small for atomic nitrogen with a radius of 0.74 Å or the still larger N ion. The estimated effective radius of nitrogen in ϵ-Fe_xN of 0.68 Å is consistent with the view that interstitial nitrogen (and by similar argument, carbon, too) donates electrons and exists in the structure as positively charged ions.

retention of about 15% interstitial N in the stabilized Fe-C-N catalyst [19] should therefore result in a slightly larger electron population in the iron d band than in the corresponding Fe-carbide. In sum, then, one should be able to consider the promotional properties of nitrogen in much the same vein as those of potassium, and the net effects of both in terms of electron donation to iron could well be approximately additive.

IRON-MANGANESE

The iron-manganese system, at least in unsupported form, has been claimed to be an efficient producer of low molecular weight olefins [29,30]. A detailed summary of the catalytic activity and selectivity properties of these materials will not be given here (these are available in a number of different sources [31–39]); whether FeMn is indeed a good olefin catalyst is still subject to discussion. The system is, however, an extremely complex and very interesting one both from the point of reactivity/selectivity and materials characterization, and some aspects of this are covered here, based primarily on the extensive studies of Baerns and co-workers. *

The major information derives from a series of four catalysts, A-(97% Fe, 3% Mn), B-(85% Fe, 15% Mn), C-(40.3% Fe, 59.7% Mn) and D-(19.1% Fe, 80.9% Mn) [32], examined after calcination in an inert atmosphere at 500°C, after reduction, H_2, 24 h (various temperatures), and after synthesis (270°C, $P_{CO} = 2.75$ bar, $P_{H_2} = 5.5$ bar, 200 h).

The phase compositions are characterized as to whether the catalysts are iron rich (A and B) or manganese rich (C and D). For the *iron-rich* materials, after heating in inert at 500°C a single phase solid solution of Mn in hematite, α-$(Fe_{1+x}Mn_x)_2O_3$ is formed; reduction at 400°C, 24 h yields essentially unalloyed metallic iron with only trace quantities of dissolved Mn, and about 15% of a wustite phase (probably containing dissolved Mn [31]). The phase composition of "reduced" materials is rather sensitive to the temperature employed; after H_2, 300°C, 24 h only about 20% of the iron is present as unalloyed metal, about 60% as a manganospinel $(Fe_{1-y}Mn_y)_3O_4$ with $0.1 < y < 0.2$, and about 20% unreduced parent α-$(Fe_{1-x}Mn_x)_2O_3$. Overall, one can postulate the following sequence for the reduction:

$$\alpha\text{-}(Fe_{1-x}Mn_x)_2O_3 \rightarrow (Fe_{1-y}Mn_y)_3O_4 \rightarrow (Fe_{1-z}Mn_z)O \rightarrow Fe + MnO$$

with a separation of Fe and MnO occurring in the last stage. The phase composition of the used catalyst also depends on the temperature of reduction. In general, after synthesis the catalyst is a triphasic material containing $(Fe_{1-y}Mn_y)_3O_4$ with $-y \sim 0.05$, ϵ'-$Fe_{2.2}C$ and χ-Fe_5C_2, with very little Mn dissolved in the carbide phases. For 400°C reduction, there is less spinel and

* We here deviate from the separation of Parts I and II into "Characterization" and "Reactivity". However, for the FeMn system there seems to be no convenient way to do this otherwise.

Table 2
Phase composition of a Fe-rich Fe-Mn catalyst after synthesis

Initial composition	T_R (°C)	% of total		
		$(Fe_{1-x}Mn_x)_3O_4$	ϵ'-$Fe_{2.2}C$	χ-Fe_5C_2
97% Fe, 3% Mn	300	71	19	10
97% Fe, 3% Mn	400	55	13	32

more carbide compared to 300°C reduction, and also a greater relative amount of χ carbide compared to ϵ'-carbide. Typical compositions are shown in table 2 for catalyst A of the series. The phase changes during synthesis are not simple: The 300°C reduction catalyst starts with 20% metallic iron and ends up with 29% carbide, while the 400°C catalyst starts with more than 85% metallic iron and ends up with only 45% carbide. This suggests competing oxidation, reduction and carburization during synthesis.

For the *manganese-rich* catalysts the phase distributions are at least as complex and are more inhomogeneous. After the 500°C treatment the starting material is biphasic with an iron-rich α-$(Fe_{1-x}Mn_x)_2O_3$ phase and a manganese-rich cubic β-$(Mn_{1-y}Fe_y)_2O_3$ having a bixbyite structure with $y = 0.3$. The relative amounts of the Mn-rich phase is about 40% for C and 80% for D. Also, these catalysts after reduction and/or use have a nonmagnetic oxide phase containing Fe^{3+} not seen in iron-rich materials.

Thus, as compared to the α-phase, the Mn-rich phase is more difficult to reduce, but the reduced iron is still found to be nearly unalloyed and so are the carbides. Earlier observations regarding the dependence of Fe-rich spinel/carbide and χ-Fe_5C_2/ϵ'-$Fe_{2.2}C$ ratios on temperature of reduction hold true for the Mn-rich catalysts also. Thus there is a much smaller amount of Fe-rich spinel, and larger amount of carbide and larger χ/ϵ' ratio for 400°C reduction. The amount of iron in the wustite phase is in a narrow range of 25–35% and does not depend significantly on the temperature of reduction.

Unlike catalysts A and B, the spinel phase found in catalysts C and D has an extremely inhomogeneous composition. Part of the spinel is close to Fe_3O_4 whereas some other parts have Mn concentrations as high as in $FeMn_2O_4$. It is quite likely that the inhomogeneous spinel $Fe_{3-y}Mn_yO_4$ has values of y ranging from 0 to 2.

From the equilibrium phase diagram of the Fe_2O_3–Mn_2O_3 system as reported in the literature [40,41] one would expect a single phase β-$(Mn_{1-y}Fe_y)_2O_3$ material for the samples with 40% and 20% Fe content (i.e., C and D). The calcination at 500°C for 24 hours is insufficient to equilibrate the system, because there are two phase mixtures. Both catalysts C and D were also calcined at 1050°C for 36 hours. Indeed a single β-phase material was found for D, while the amount of α-phase for C decreased to a small value (about 10%).

The effects of structure or phasic composition on FT activity/selectivity are difficult to render on a quantitative basis for these catalysts, since they are so complex. This is particularly so for the Mn-rich materials. For example, in catalysts C and D the starting material consists of two phases: the Fe-rich α-phase and the Mn-rich β-phase. These two phases are reduced to different extents and to different crystallographic phases, which leaves a four component catalyst at the start of the synthesis reaction. It is hard to figure out structure-related catalytic effects from this kind of material.

However, a few general observations can still be made by looking at activity patterns and Mössbauer analysis. First, and probably most importantly, the differences in the activity-selectivity of various catalysts apparently have nothing to do with electronic alloying effects, because the metallic and the carbide phase are unalloyed by Mn. The concentration of dissolved Mn in the metal and carbides is undetectable even when the overall Mn content of the catalyst is 80%. This is unlike Fe-Co and Fe-Ni mixed catalysts where extensive alloying is known to take place on calcination and reduction [1].

There is some correlation between the phase distribution and activity pattern for samples A and B. In the beginning of the synthesis a high initial metallic Fe-content for the samples reduced at higher temperature is related with the higher activity and selectivity towards C_2 to C_4 olefins, as compared to the catalyst reduced at lower temperature. With increasing time on stream the activity of the catalyst reduced at higher temperature decreases while that of the catalyst reduced at lower temperature increases. After 200 hours of synthesis both the activity and selectivity patterns have reversed. It would appear that the different amount of the total carbide and the ratio of χ to ϵ'-carbide could be responsible for this behavior. In any event, the interpretation of activity and selectivity patterns, and the role of carbide formation, appears to be similar to iron catalysts for the iron-rich FeMn (at least to $\sim$ 20% Mn). It remains unexplained why low temperature reduction of these catalysts leads to more ϵ'-carbide and high temperature reduction to more χ-carbide, and this was not a topic investigated in any detail for supported Fe. A speculation is that there is a larger fraction of large Fe particles after 400°C reduction (via sintering or reduction kinetics), and these are known to form χ-Fe_5C_2 more easily. In fact the extent of χ-carbide formation after 400°C reduction here ($\sim$ 32%) is comparable to that formed in the supported Fe catalyst after 425°C reduction and carburization under similar conditions for only 3 h ($\sim$ 45%).

Catalysts C and D show fairly similar behavior with respect to activity and olefin selectivity even after 200 h FT utilization. As stated above, these are rather inhomogeneous agglomerates of at least five phases, and little can be concluded quantitatively. Probably the structural differences originating in the α- and β-phases compensate each other and mask their intrinsic differences. It is likely that the particle size distribution and morphology of the reduced iron in the β-$(Fe_{1-x}Mn_x)_2O_3$ is important in determination of the catalytic properties of

Table 3
Distribution of Fe in the phases present in FeMn after 200 h of synthesis

Initial Fe (%)	97		85		40.3		19.1	
Reduction T (° C)	300	400	300	400	325	375	300	400
1. Carbides	10	32	–	80	–	31	–	44
2. Magnetic Fe-rich Spinel $(Fe_{1-x}Mn_x)_3O_4$	71	55	93	15	38	28	21	–
3. Fe^{3+}-oxide (nonmagnetic Mn-rich spinel)	–	–	–	–	23	17	31	20
4. Fe^{2+}-oxide (Wüstite)	–	–	–	–	31	24	27	36

Mn-rich catalysts, but this material has not been investigated separately. Table 3 presents a summary of these characterizations for this wonderfully complicated system.

4. Summary

A dispassionate observer would probably conclude that this survey of reaction results on iron and iron-based alloy catalysts leaves us pretty much in the same place as at the end of Part I. In spite of the large amount of work and the diversity of systems examined, the exact definition of the role of carbide phases in Fischer-Tropsch synthesis on these catalysts remains elusive. It is probably fair to say that nowhere in these examples has it been established without question that iron carbide, in any of its many forms, provides directly an active site for the synthesis that can be associated with the formation of a particular product or class of products. There are possible electronic promotion effects resulting from carbide formation that are similar to those provided by potassium or nitrogen, and that are also seen in some of the alloys where no carbide is formed such as FeCo. In other alloys such as FeMn, where carbide phases are readily formed and detected, the solid state tranformations become so complex as to preclude the possibility of any direct correlations.

As stated in Part I, the initial activation of reduced iron seems directly correlated with the formation of a carbide phase, but it can be argued with reason that this is more a promotion than a geometric (i.e., site formation) effect. The majority of the evidence both from characterization and reaction studies points to

the role of carbide phases as involved spectators who have an indirect influence on the outcome of the game.

Acknowledgment

The bulk of the work at Northwestern University described was conducted with support from the Department of Energy, Office of Basic Energy Sciences (Contract DE-AC02-78ERO-4993) and Pittsburgh Energy Technology Center (Grant DE-FG22-83PC-60795) in collaboration with Professors L.H. Schwartz and P.C. Stair. Work joint with the Ruhr-Universität Bochum was supported by the NATO Collaborative Research Grants program (Grant RG.117.81) and the Alexander von Humboldt-Stiftung in collaboration with Professor M. Baerns and Dr. H. Papp.

References

[1] J.A. Amelse, L.H. Schwartz and J.B. Butt, J. Catal. 63 (1981) 95.
[2] R.B. Moyes and M.W. Roberts, J. Catal. 49 (1977) 216.
[3] H.H. Podgurski, J. Kummer, T. Dwtitt and P.H. Emmett, J. Am. Chem. Soc. 72 (1950) 5382.
[4] E. Unmuth, L.H. Schwartz and J.B. Butt, J. Catal. 63 (1980) 404.
[5] J.A. Amelse, J.B. Butt and L.H. Schwartz, J. Phys. Chem. 82 (1978) 558.
[6] G.B. Raupp and W.N. Delgass, J. Catal. 58 (1979) 348, 361.
[7] D.J. Dwyer and G.A. Somorjai, J. Catal. 52 (1978) 291; 56 (1978) 249.
[8] C.S. Kuivila, P.C. Stair and J.B. Butt, J. Catal. 118 (1989) 299.
[9] K.B. Arcuri, L.H. Schwartz, R.D. Piotrowski and J.B. Butt, J. Catal. 85 (1984) 349.
[10] R.B. Anderson, in: *Catalysis*, ed. P.H. Emmet, Vol. IV (Reinhold, NY, 1956).
[11] H.E. Atwood and C.O. Bennett, I.E.C. Proc. Design Devel. 18 (1979) 163.
[12] M.E. Dry, IEC Prod. Res. Devel. 15 (1976) 282.
[13] J.W. Niemanstverdriet, A.M. van der Kraan, W.J. van Dijk and H.S. van der Baan, J. Phys. Chem 84 (1980) 3363.
[14] J.M. Driessen, E.K. Poels, J.P. Hindermann and V. Ponec, J. Catal. 82 (1983) 26.
[15] J.B. Butt, L.H. Schwartz, M. Baerns and R. Malessa, IEC Prod. Res. Devel. 23 (1984) 51.
[16] K.H. Jack, Proc. Roy. Soc. London, Ser. A 195 (1948) 34.
[17] K.H. Jack, Acta Crystallogr. 5 (1952) 404.
[18] G.M. Chen, N.K. Jaggi, J.B. Butt, E.G. Yeh and L.H. Schwartz, J. Phys. Chem. 87 (1983) 5326.
[19] E. Yeh, N.K. Jaggi, J.B. Butt and L.H. Schwartz, J. Catal. 91 (1985) 231.
[20] D.H. Jack and K.H. Jack, Mater. Sci. Engr. 11 (1973) 1.
[21] R.B. Anderson, Catal. Rev.-Sci. Engr. 21 (1980) 53.
[22] E.H. Yeh, L.H. Schwartz and J.B. Butt, J. Catal. 91 (1985) 241.
[23] R.B. Anderson, J.F. Schultz, B. Seligman, W.K. Hall and H.H. Storch, J. Am. Chem. Soc. 72 (1950) 3502.
[24] M.E. Dry, T. Shingles, L. Boshoff and A. Vosthuisen, J. Catal. 15 (1969) 190;
see also M.E. Dry and G.J. Oosthuizen, J. Catal. 11 (1968) 18.
[25] K.H. Eickel and W. Pitsch, Phys. Status Solidi 39 (1970) 121.
[26] R.J. Bouchard, C.G. Frederick and V. Johnson, J. Appl. Phys. 45 (1974) 4067.

[27] G.W. Weiner and J.A. Berger, J. Metals 7 (1955) 360.
[28] G. LeCaer, J.M. Dubois, M. Pijolat, V. Perrichon and P. Bussiere, J. Phys. Chem. 86 (1982) 4799.
[29] H. Kölbel and K.D. Tillmetz, Deutsche Offen.; 2,507,647 (1976).
[30] B. Büssemeier, C.D. Frohning, G. Horn and W. Kluy, Deutsche Offen.; 2,518,964 (1976).
[31] N.K. Jaggi, L.H. Schwartz, J.B. Butt, H. Papp and M. Baerns, Appl. Catal. 13 (1985) 347.
[32] G.C. Maiti, R. Malessa and M. Baerns, Appl. Catal. 5 (1983) 151.
[33] C.N. Satterfield and H.G. Stenger, IEC Proc. Design Devel. 23 (1984) 26.
[34] J. Barrault, C. Forquy and V. Perrichon, Appl. Catal. 5 (1983) 119.
[35] G.C. Maiti, R. Malessa, U. Löchner, H. Papp and M. Baerns, Appl. Catal. 16 (1985) 215.
[36] K.B. Jensen and F.E. Massoth, J. Catal. 92 (1985) 98.
[37] W.D. Deckwer, Y. Serpemen, M. Ralek and B. Schmidt, IEC Proc. Design Devel. 21 (1982) 222.
[38] K.M. Kreitman, M. Baerns and J.B. Butt, J. Catal. 105 (1987) 319.
[39] J. Venter, M. Kaminsky, G.L. Geoffroy and M.A. Vannice, J. Catal. 105 (1987) 155.